Available online at www.sciencedirect.com
ScienceDirect
Acta Materialia 58 (2010) 3068–3072
Acta MATERIALIA
www.elsevier.com/locate/actamat

Broadband anti-reflection and enhanced field emission from catalyst-free grown small-sized ITO nanowires at a low temperature

Neng Wan, Jun Xu *, Guran Chen, Xinhui Gan, Sihua Guo, Ling Xu, Kunji Chen

Nanjing National Laboratory of Microstructures, Jiangsu Provincial Key Laboratory of Photonic and Electronic Materials Sciences and Technology, School of Physics and School of Electronic Science and Technology, Nanjing University, Nanjing 210093, People's Republic of China

Received 6 November 2009; received in revised form 25 January 2010; accepted 25 January 2010
Available online 18 February 2010

Abstract

Small-sized indium tin oxide (ITO) nanowires were fabricated using the electron beam evaporation (EBE) technique at low temperature (~150 °C) without adding any catalyst. The ITO nanowires have a typical diameter of around 10 nm and a length of more than 100 nm, with body-centered cubic crystal structures that grow along the ⟨1 0 0⟩ directions, as revealed by transmission electron microscopy. The growth mechanism of the branched ITO nanowires was found to be a vapor–solid process. The nanowire films show a broadband anti-reflection property due to the graded refraction index from the film surface to the substrate. Enhanced field emission properties with a low turn-on electric field and a high field enhancement factor were also observed in the ITO nanowires.

Keywords: ITO; Nanostructure; e-Beam evaporation; Field emission; Anti-reflection

1. Introduction

One-dimensional (1-D) metal–oxide nanostructures are currently the subject of much interest both for their novel structures and physical properties and for their potential applications in nanoelectronics and nanophotonics [1–3]. Many kinds of 1-D oxide, such as ZnO and SnO_2, have been fabricated and studied. As one of the most important and widely used materials, tin-doped indium oxide (ITO) has been applied in various devices, such as light-emitting devices, sensors and solar cells [4–7]. It has been reported that 1-D ITO nanostructures can be prepared by many kinds of techniques. For example, by using a carbothermal evaporation method, Chiquito et al. [8] were able to obtain ITO 1-D nanobelts with a thickness of around 60 nm and a length of several microns at a temperature of 1150 °C through the vapor–solid (VS) process, and novel electrical transport properties were found. Wan et al. [9] used the Au-catalyzed vapor–liquid–solid (VLS) route to obtain ITO nanowires in a pulsed laser deposition system. Because the Au catalyst was used, the preparation temperature could be decreased greatly to 600 °C. The nanowires had a diameter of <200 nm and a length of about 2.5 μm. Good field emission behavior was observed in the nanowires due to the high aspect ratio and the highly aligned geometry. More recently, O'Dwyerl et al. [10] reported the fabrication of ITO nanowires at 500–600 °C by using a molecular beam evaporation method through the VLS route. In–Sn droplets were used as the catalyst in the deposition process, and the ITO nanowires had diameters of 8–20 nm and lengths of 40–500 nm, which were used as the transparent conduction electrode in the electroluminescence devices to enhance the emission efficiency [10].

The conventional thermal evaporation and condensation process usually requires a high temperature (~1000 °C). Catalyzed growth, on the other hand, can be performed at a temperature of ~500–600 °C. However, the use of the catalyst may cause contamination by extra elements, which may cause a deterioration in the properties of the applications [1]. As a result, the fabrication of ITO nanostructures at low temperature with low cost and enhanced properties is currently a very attractive goal. Moreover, the formation

* Corresponding author.
E-mail address: junxu@nju.edu.cn (J. Xu).

1359-6454/$36.00
doi:10.1016/j.actamat.2010.01.041

of ultrathin 1-D nanowires (<10 nm) is also of interest as decreasing the diameter will increase the surface area and colloidal stability, which can have repercussions on applications [11]. Here, we report the growth of single-crystal ITO nanowires over a large area using a low-temperature process (~150 °C) in an e-beam evaporation system without adding any catalyst. The approach used in the present work has the advantage of low cost, high uniformity and good reproducibility. The diameter of the ITO nanowire is around 10 nm and the length is longer than 100 nm. Moreover, enhanced field emission and broadband anti-reflection characteristics were observed in the ITO nanowires, which indicates the potential application of these films in future optoelectronic devices.

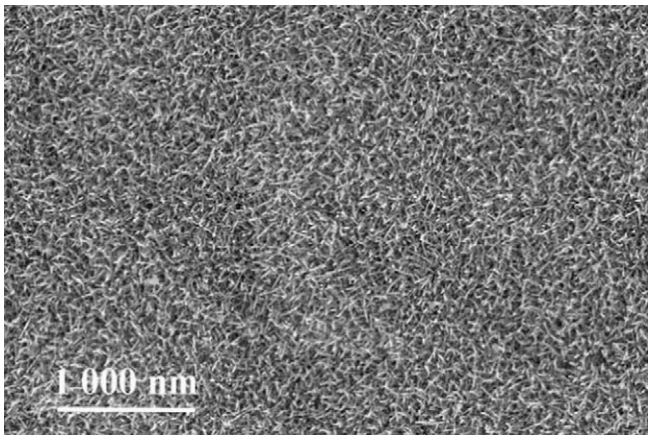

Fig. 1. FESEM image of the ITO nanowires.

2. Experiments

ITO nanowires were prepared in a conventional e-beam evaporation system with the accelerating voltage of the e-beam set at 6 keV. Before the evaporation process, the chamber was pumped down to a base pressure of $<10^{-4}$ Pa. The substrate temperature was 150 °C and ITO ceramic pellets with an In/Sn molar ratio of 85/15 were used to grow ITO nanowires without introducing any extra atmosphere. The growth of the flat ITO films was performed at <150 °C with an In/Sn molar ratio of 95/5 and an oxygen pressure of 2.7×10^{-2} Pa. In order to improve the film's uniformity, the sample holder was rotated at a speed of 30 rpm. Si wafer and aluminum foil were used as substrates. It is worth pointing out that neither catalyst nor template was used during the preparation process.

The microstructure of the ITO nanowires was characterized by field emission scanning electron microscopy (FESEM; LEO 1530VP, Zeiss) and field emission transmission electron microscopy (TEM; TECNAI F20, FEI). The composition of the nanostructures was determined using the electron energy dispersion spectra (EDS) in the TEM system, which worked under the scanning transmission electron microscopy mode. The optical transmission and reflection were measured using a Shimadzu UV-3600 spectrometer. The transmission spectra (T) were obtained under normal incidence geometry and the reflection spectra (R) were obtained under 5° mirror reflection geometry, using an aluminum mirror with a smooth reflection dependence in the measured wavelength region as the reference. The field emission measurement was performed in a vacuum chamber at room temperature, with the pressure at less than 1×10^{-4} Pa. The emitting area was 7 mm × 7 mm and the cathode–anode distance was about 280 μm. During the measurements, the applied voltage was ramped up and down for several cycles until the stable field emission behavior was obtained.

3. Results and discussion

Fig. 1 shows a typical FESEM image of synthesized ITO nanowires. As seen in the figures, the ITO nanowires have good uniformity in a large area with high density. The ITO nanowires have an average diameter in the sub-10 nm range, with a length larger than 100 nm. The morphologies and structures were further investigated by planar and side-view TEM images, as shown in Fig. 2a and b, respectively. It can also be seen from the TEM images that the diameter of the ITO nanowires is quite uniform. The ITO nanowires are seen to be straight, and some of them have branches. The branches have grown perpendicular to the truck along all four possible directions, and adjacent branches are perpendicular to each other. This structure is illustrated in the inset of Fig. 2b. It is also noted that the ITO nanowires have the

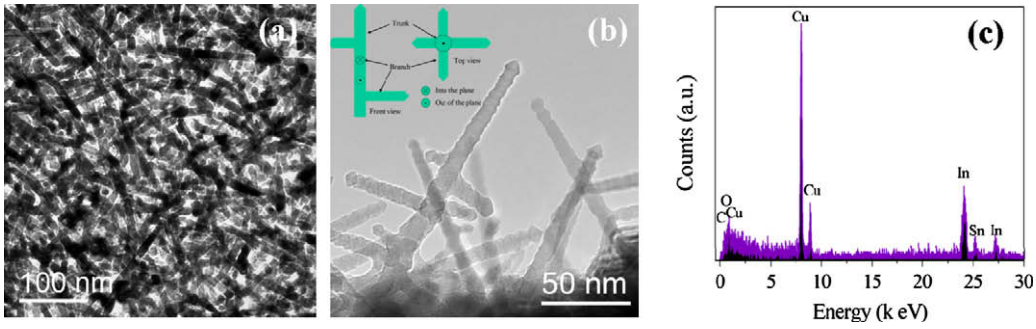

Fig. 2. (a) Planar view and (b) side view of the TEM image of the ITO nanowires; (c) the EDS spectrum of the ITO nanowires. The inset in (b) is a schematic figure showing the orientation of the branches grown on the nanowire trunks.

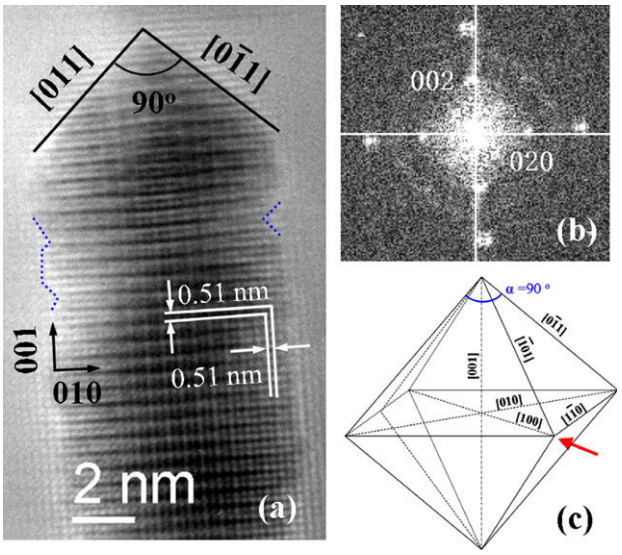

Fig. 3. (a) HRTEM image at the tips of the ITO nanowire obtained along the zone axis of ⟨1 0 0⟩; (b) FFT image of the HRTEM image; and (c) the octahedron of the bcc structure with indexed crystal orientations. The red arrow indicates the observation direction. (For interpretation of the references to colour in this figure legend, the reader is referred to the web version of this article.)

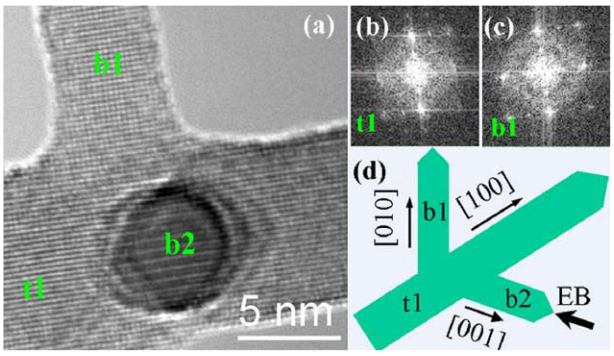

Fig. 4. (a) HRTEM image at the branch region of the ITO nanowire obtained along the ⟨1 0 0⟩ direction. The labels b1 and b2 stand for the two branches; t1 stands for the trunk. (b and c) FFT patterns obtained at the trunk "t1" and branch "b1". (c) Schematic three-dimensional structure corresponding to the morphology observed in (a). EB stands for the illuminate direction of the e-beam.

faceted tips and facets sidewalls. Fig. 2c shows the EDS of the ITO nanowires. The signals from In and Sn can be well resolved from the figure. The signals from Cu and C arise from the copper mesh and the carbon film-coated TEM sample sustaining substrate. The In/Sn ratio was estimated to be 4, which is lower than the target material. We attributed this deviation in the In/Sn ratio to the preferred evaporation of Sn during the e-beam evaporation process since its boiling point is lower than that of In.

The high-resolution TEM image shown in Fig. 3a reveals that the synthesized ITO nanowires have a single crystal nature with body-centered cubic (bcc) structures. The lattice parameter identified in Fig. 3a is 0.51 nm, which suggests that the growth direction is ⟨1 0 0⟩. The fast Fourier transformation (FFT) pattern of the nanowire given in Fig. 3b shows clear dots corresponding to the (1 0 0) planes, indicating that the nanowire is well crystallized. According to the TEM results, the ITO nanowires grow along the ⟨1 0 0⟩ directions and their tips have {1 1 1} faces and ⟨1 1 0⟩ ridges. The observation of the 90° angle at the nanowire tips, as indicated in the TEM image, is also schematically interpreted according to Fig. 3c.

We investigated the influence of various substrates on the formation of the ITO nanowires. It was found that ITO nanowires can be grown on various substrates, such as Si wafer, glass and Al foil, with the same morphologies and structures, indicating that the preparation of ITO nanowires is not dependent on the substrate material or crystal structures in our case.

The branched ITO nanowires were also investigated by high-resolution TEM. As shown in Fig. 4a, two branches grew on the trunk of the ITO nanowires, labeled as b1 and b2, respectively (t1 represents the ITO trunk). It is clearly shown that the branches grew perpendicular to the trunk, and that the two branches are normal to each other. The branches can be identified as being single crystalline, with the same lattice fringes, and there are no defects or mismatches in the interfacial region between the branches and the trunk, suggesting epitaxic growth in all the directions.

It has been reported that the 1-D nanostructures can be prepared via either the VLS or the VS mechanism [12–14]. In our case, neither the catalyst nor the templates were used during the preparation process. Moreover, we could not find any separate low melting parts on the tips of nanowires, as verified by the TEM investigations. Therefore, we tentatively suggest the growth of ITO nanowires in our case is likely through the VS mechanism, which means that the vapor species condensed directly on the substrates to form the ITO nanowires. Fig. 5 presents a schematic diagram to further explain the growth and branching mechanism of ITO nanowires, which is easy to interpret and correlates with the experimental observations.

ITO films have been widely used as a transparent conduction oxide in solar cells and light-emitting diodes. Since the refraction index of ITO films is about 2.0, there is a sharp change in the refraction index at the ITO film/air interface,

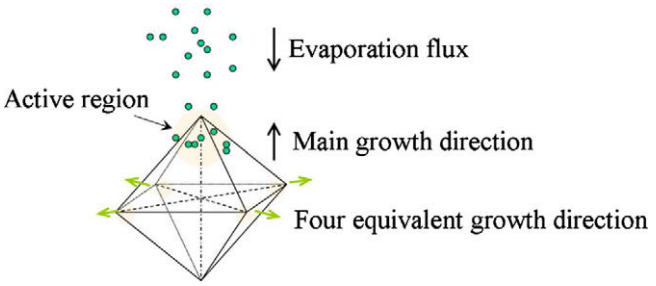

Fig. 5. Model for the interpretation of the growth process of the branched ITO nanowires. The octahedron stands for the bcc structures of ITO, which act as the growth core.

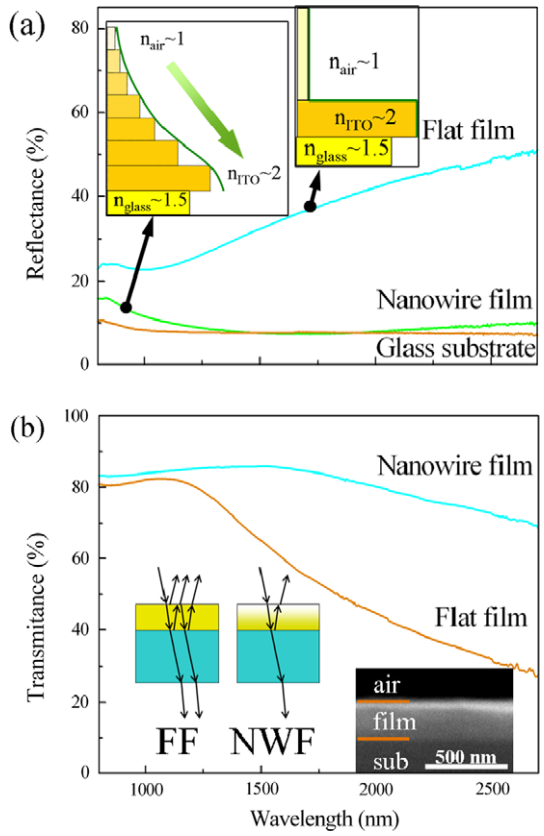

Fig. 6. Reflection (a) and transmission (b) spectra of the flat and nanowire film. The inset in (a) shows the refraction index profile of the nanowire (left side) and the flat (right side) film. Inset in (b): left side, the different situation of light transmission and reflection in the flat film (FF) and the nanowire film (NWF); right side, the cross-sectional SEM image of the flat film.

as depicted in the insert of Fig. 6a (right side), which causes remarkable light reflection. Previous works have demonstrated that a gradually changing refraction index from the surface is beneficial for anti-reflection [15–18]. One of the best methods for the formation of a graduated refraction index is to change the filling factor from the film surface to the film/substrate, as illustrated in the inset of Fig. 6a (left side). In this case, it is able to efficiently eliminate the reflected light across a wide spectrum due to the refraction index matching.

The reflection (R) and transmission (T) of the ITO nanowire after 350 °C annealing are presented in Fig. 6a and b. For comparison, the corresponding curves of the flat surface ITO film are also shown in the same figure. A cross-sectional SEM image of the flat film is shown in the inset of Fig. 6b for reference. We note here that annealing at 350 °C only affects the morphology of the ITO nanowires slightly, but it can reduce the absorption by defects in the as-deposited samples. As shown in Fig. 6a, the flat film shows high reflectance across the whole measured region, especially in infrared region ($R > 20\%$), while the nanowire film shows evidence of broadband anti-reflection. The reflectivity is around 10% from 800 to 3000 nm, which is comparable to the bare substrate. The transmittance spectra of the two kinds of film are also presented in Fig. 6b, where the ITO nanowires show significantly improved transmittance, with the transmittance being above 70% across the whole measurement range. The broadband anti-reflection can be attributed to the graded refraction index due to the gradual change in the filling factor from the bottom to the top surface of the film, as discussed before. As shown in Figs. 1 and 2b, the filling factor of the ITO material gradually decreases from the surface to the interface due to the non-aligned growth of the ITO nanowires. There are more ITO nanowires, with branches growing at different angle, which results in more ITO nanowires growing near the substrate surface. Thus, the inner reflection at the film/substrate and film/air interfaces will be reduced, thus causing the anti-reflection effect (see inset in Fig. 6b). The significant decrease in the reflectance and increase in the transmittance suggests that it is crucial in the application of highly efficient semiconductor solar cells.

One-dimensional nanostructures usually have good field emission characteristics [2]. Fig. 7 shows the emission current density (J) as a function of the applied electric field (E) for a ITO nanowire sample and a reference flat ITO sample, respectively. As seen in the figure, the current density increases as the applied electric field is elevated for both samples, and the ITO nanowire film shows obviously enhanced field emission characteristics. The turn-on electric field at a current density of 1 μA cm^{-2} is about 4.5 V μm^{-1} for the ITO nanowire film, while it is about 12.5 V μm^{-1} for the flat surface ITO film. The inset of Fig. 7 shows the Fowler–Nordheim (F–N) plot by fitting the field emission characteristics according to the relationship [9]:

$$Ln\left(\frac{J}{E^2}\right) = -\frac{b\phi^{3/2}}{\beta}\left(\frac{1}{E}\right) + Ln\left(\frac{a\beta^2}{\phi}\right), \quad (1)$$

where $a = 1.54 \times 10^{-6}$ A eV/V^2, $b = 6.83 \times 10^9$ V m^{-1} eV$^{3/2}$, ϕ is the work function of ITO material (here, we choose

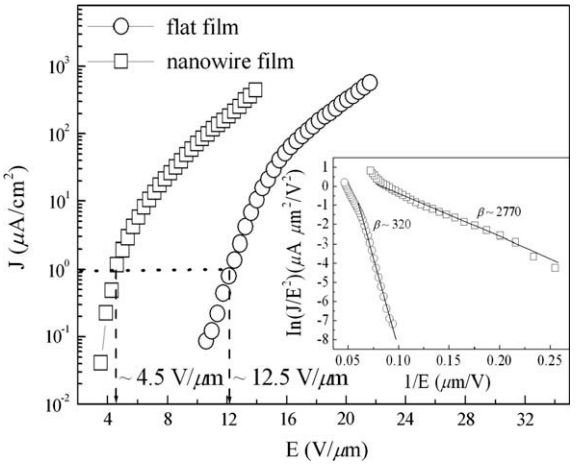

Fig. 7. Field emission current density (J) as a function of applied electric field (E) for the flat film and nanowires. The inset shows the Fowler–Nordheim plots for both samples.

$\phi = 4.3$ eV) [9], E is the applied electric field and β is the field enhancement factor. As shown in the figure, the field emission data can be fitted well by the F–N relationship for both samples, indicating that the quantum tunneling mechanism dominates in the electron emission process. The field enhancement factor β can be estimated from the slope of the F–N plots, which is found to be 2770 for the ITO nanowire film and 320 for the flat surface ITO film, respectively.

It is known that the reduced turn-on electric field and the large field enhancement factor can be caused by the lowering of the work function and the formation of a high aspect ratio structure [19]. According to previous works, the change in the In/Sn ratio and the oxygen content in the ITO material will cause the work function to change by less than 0.8 eV [20,21], which could be the reason for the enhanced field emission property. From another angle, the ITO nanowires have a length of >100 nm and a diameter of <10 nm, which means that the aspect ratio is larger than 10. The high aspect ratio plays an important role in enhancing the field emission characteristics, since the field enhancement factor is proportional to the aspect ratio of the emitters, as reported previously [22]. However, the ITO nanowires are not vertically aligned, as seen in the cross-sectional TEM image, which suggests that further improvements in the field emission properties could be achieved by preparing better aligned ITO nanowires.

4. Conclusions

In conclusion, ITO nanowires with sub-10 nm diameter were prepared at low temperature (150 °C) without using any catalyst by using the electron beam evaporation method. The nanowires have a length of several hundred nanometers with a single crystal bcc structure. The growth and branching directions of the nanowire are found to be along the $\langle 1\,0\,0\rangle$ directions. A VS growth mechanism is proposed to interpret the formation of the ITO nanowires. The ITO nanowires show a broadband anti-reflection property in the 800–3000 nm region, which reduces the reflection to around 10%. The ITO nanowires also show enhanced field emission. The field emission enhancement factor is increased to 2770 and the turn-on electric field is reduced to 4.5 V μm^{-1} in ITO nanowires. It is realized that the anti-reflection and enhanced field emission are related to the formation of the high density and high aspect ratio ITO nanowires. The significant property improvements indicate the potential applications of prepared 1-D nanowires in nanodevices.

Acknowledgements

The authors thank Mrs. Xiaoning Zhao for her assistance with the TEM. This work is supported by the “973” Project (2007CB613401) and NSF of China (10874070, 50872051 and 60721063).

References

[1] Wang ZL. ACS Nanotech 2008;2:1987.
[2] She JC, Xiao ZM, Yang YH, Deng SZ, Chen J, Yang GW, et al. ACS Nanotech 2008;2:2015.
[3] Hsin CL, He JH, Lee CY, Wu WW, Yeh PH, Chen LJ, et al. Nanotech Lett 2007;7:1799.
[4] Zhao Y, Zhang Z, Wu Z, Dang H. Langmuir 2004;20:27.
[5] Veinot JGC, Yan H, Smith SM, Cui J, Huang Q, Marks TJ. Nanotech Lett 2002;2:333.
[6] Zhang D, Liu Z, Li C, Tang T, Liu X, Han S, et al. Nanotech Lett 2004;4:1919.
[7] Hamberg I, Granqvist CG. J Appl Phys 1986;60:R123.
[8] Chiquito AJ, Escote MT, Orlandi MO, Lanfredi AJC, Leite ER, Longo E. Physica B 2007;400:243;
Chiquito AJ, Lanfredi AJC, de Oliveira RFM, Pozzi LP, Leite ER. Nanotech Lett 2007;7:1439;
Chiquito AJ, Lanfredi AJC, Leite ER. J Phys D: Appl Phys 2008;41:045106.
[9] Wan Q, Feng P, Wang TH. Appl Phys Lett 2006;89:123102.
[10] O’Dwyer1 C, Szachowicz M, Visimberga G, Lavayen V, Newcomb SB, Sotomayor Torres CM. Nat Nanotech 2009;4:239.
[11] Cademartiri L, Ozin GA. Adv Mater 2009;21:1013–20.
[12] Wang YW, Schmidt V, Senz S, Gösele U. Nat Nanotech 2006;1:186.
[13] Hao YF, Meng GW, Ye CH, Zhang LD. Cryst Growth Des 2005;5:1617.
[14] Wang M, Li D-W, Shu D-J, Bennema P, Mao Y-W, Pan W, et al. Phys Rev Lett 2005;94:125505.
[15] Lee C, Bae SY, Mobasser S, Manohara H. Nanotech Lett 2005;5:2438.
[16] Xi J-Q, Martion, Schubert F, Kimi JK, Schubert EF, Chen MF, Lin S-Y, Liu W, Smart JA. Nat Photonics 2007;1:176.
[17] Walheim S, Schäffer E, Mlynek J, Steiner U. Science 1999;28:520.
[18] Zhu J, Yu ZF, Burkhard GF, Hsu C-M, Connor ST, Xu YQ, et al. Nanotech Lett 2009;9:279.
[19] Xu J, Mei J, Huang XH, Li X, Li Z, Li W, et al. Appl Phys A 2005;80:123.
[20] Sugiyama K, Ishii H, Ouchi Y, Seki K. J Appl Phys 2000;87:295.
[21] Lin Y-J, Chen Y-M, Wang Y-C. J Appl Phys 2005;97:083702.
[22] Buldum A, Lu JP. Phys Rev Lett 2003;91:236801.